JOURNAL OF AGRICULTURAL AND FOOD CHEMISTRY

pubs.acs.org/JAFC Article

Lipid Peroxide-Derived Short-Chain Aldehydes are Involved in Aluminum Toxicity of Wheat (*Triticum aestivum*) Roots

Xin Liang, Yiqun Ou, Hongcheng Zhao, Weiwei Zhou, Chengliang Sun, and Xianyong Lin*

Cite This: *J. Agric. Food Chem.* 2021, 69, 10496−10505 Read Online

ACCESS | Metrics & More | Article Recommendations | Supporting Information

ABSTRACT: Lipid peroxidation is a common event during aluminum (Al) toxicity in plants, and it generates an array of aldehyde fragments. The present study investigated and compared the profile and physiological functions of lipid peroxide-derived aldehydes under Al stress in two wheat genotypes that differed in Al resistance. Under Al stress, the sensitive genotype Yangmai-5 suffered more severe plasma membrane damage and accumulated higher levels of aldehydes in roots than the Al-tolerant genotype Jian-864. The complementary use of high-resolution mass spectrometry and standard compounds allowed the identification and quantification of 13 kinds of short-chain aldehydes sourced from lipids in wheat roots. Among these aldehydes, acetaldehyde, isovaldehyde, valeraldehyde, (*E*)-2-hexenal (HE), heptaldehyde, and nonyl aldehyde were the predominant species. Moreover, it was found that HE in the sensitive genotype was over 2.63 times higher than that in the tolerant genotype after Al treatment. Elimination of aldehydes using carnosine rescued root growth inhibition by 19.59 and 11.63% in Jian-864 and Yangmai-5, respectively, and alleviated Al-induced membrane damage and protein oxidation. Exogenous aldehyde application further inhibited root elongation and exacerbated oxidative injury. The tolerant genotype Jian-864 showed elevated aldehyde detoxifying enzyme activity and transcript levels. These results suggest that lipid peroxide-derived short-chain aldehydes are involved in Al toxicity, and a higher aldehyde-detoxifying capacity may be responsible for Al tolerance.

KEYWORDS: *aluminum, wheat, short-chain aldehydes, toxicity, tolerance, detoxification*

Downloaded via ZHEJIANG UNIV on September 15, 2021 at 11:23:39 (UTC).
See https://pubs.acs.org/sharingguidelines for options on how to legitimately share published articles.

INTRODUCTION

Aluminum (Al) is the most abundant metal element in Earth's crust, and it is generally present in nontoxic aluminosilicates and oxides in soils.[1−3] When the soil pH value drops below 5.0, soluble Al^{3+} ions are released and become phytotoxic to plants.[1,2] Al toxicity is one of the primary factors limiting plant growth and productivity in acidic soils, which comprises approximately 30−40% of the world's arable land and 50−70% of the world's potentially arable land.[1,4] Under Al exposure, the root apex is the primary site in the perception and manifestation of Al toxicity.[1,5] At the cellular level, high Al accumulation in root cells causes callose deposition, cell wall rigidity, and signal disruption.[1,6] At the molecular level, Al stress alters the expression of a series of genes, some of which are critical in reactive oxygen species (ROS) metabolism.[4,7,8] Various studies showed that Al-triggered ROS caused irreversible and detrimental oxidative damage to cellular macromolecules, such as protein, DNA, and fatty acids.[6,7] By oxidizing polyunsaturated fatty acids, unbalanced ROS triggers sequential lipid peroxidation, which results in the formation of reactive aldehyde compounds.[9,10] ROS is generally considered the primary damaging agent, and it was extensively investigated.[11,12] However, few studies examined the biological function of lipid peroxide-derived aldehydes in plants.

Compared to ROS, lipid peroxide-derived aldehydes have a longer half-life and diffuse and transport more easily across membranes, which lead to the long-distance dispersal of oxidative damage in plants.[10,13,14] The formation of aldehydes leads to the formation of advanced lipoxidation end products (ALEs) with DNA and proteins,[15,16] which cause detrimental effects on cellular metabolism. For example, α,β-unsaturated aldehydes derived from lipid peroxides, such as acrolein, (*E*)-2-hexenal (HE), and 4-hydroxy-(*E*)-2-nonenal (HNE), with the typical chemical structure R−C═C−CHO, are highly electrophilic and extremely cytotoxic and consequently affect cell metabolism.[17,18] Recent studies revealed that adverse conditions, such as drought,[19] salt,[20] high temperature,[21] and low-nitrogen stress,[22] increase the generation of reactive aldehydes in plants. A few studies showed that lipid peroxide-derived aldehydes mediated stress-induced injury in plants. For example, intense illumination-induced acrolein and HE contributed to photoinhibition in tobacco.[23] Overexpressing reactive aldehyde detoxification enzymes reduces the abundance of lipid peroxide-derived aldehydes and confers plant tolerance to stress when ROS production is stimulated.[24−26] These reports indicate that aldehydes are not merely markers of oxidative stress but propagate oxidative stress in plant cells. Therefore, the formation and accumulation of aldehydes derived from lipid peroxidation should be strictly controlled in plant cells, especially under adverse conditions.

Received: July 2, 2021
Published: September 6, 2021

ACS Publications © 2021 American Chemical Society

https://doi.org/10.1021/acs.jafc.1c03975
J. Agric. Food Chem. 2021, 69, 10496−10505

Lipid peroxidation under Al stress was identified in various plants, such as pineapple,[27] lettuce,[28] wheat,[4] and maize.[29] However, reports on the implication of lipid peroxidation in Al toxicity are contradictory. The oxidation of lipids is responsible for Al phytotoxicity in maize, wheat, and Arabidopsis.[7,29,30] However, lipid peroxidation was not the primary cause of inhibition of root elongation in other plant species, for example, *Pisum sativum* and *Lotus corniculatus*.[31,32] Different functions of lipids derived from aldehydes in Al phytotoxicity were proposed based on the fatty acid peroxide fragmentation pathway, which generates an array of aldehyde fragments and attracts different molecular targets depending on their levels. More than a dozen species of aldehydes were found in plants,[31−33] and some of these aldehydes are enhanced under stress conditions. For example, acrolein, (*E*)-2-pentenal, and HE significantly increased in illuminated tobacco leaves, and acrolein was the most toxic product.[23] Under Al stress, malondialdehyde (MDA) is the best-known lipid oxidation product, and it was the subject of intense studies.[8,30] However, relatively little is known about the other aldehyde fragments. A previous study reported that HNE, but not MDA, was the major catabolite from lipid peroxidation in barley roots under Al stress.[34] Therefore, the characterization of individual aldehydes does not completely reflect the contribution of multiple aldehyde fragments to Al toxicity.

The present study characterized the provenance, maintenance, and biological toxicity of multiple lipid peroxide-derived aldehydes in the roots of two wheat genotypes that differed in Al tolerance. The role and function of aldehyde-detoxifying enzymes in alleviating Al toxicity and improving Al tolerance were also evaluated.

MATERIALS AND METHODS

Plant Culture and Treatments. Two wheat (*Triticum aestivum* L.) genotypes, the Al-tolerant wheat genotype Jian-864 and the Al-sensitive genotype Yangmai-5, were used. The seeds were sterilized in 1% (v/v) sodium hypochlorite solution for 20 min and then washed thoroughly and soaked in deionized H_2O for 1 day. The seeds were transferred to wet gauze and germinated at 25 °C in the dark for 24 h. The germinated seeds were transferred to a 4 L plastic culture chamber containing 0.5 mM $CaCl_2$ (pH 4.3). Seedlings were cultivated in a growth chamber at 25/22 °C with a 12/12 h photoperiod, 70% relative humidity, and a photosynthetic photon flux density of 300 μmol m^{-2} s^{-1}. After 3 days of preculture, healthy and uniform seedlings were selected and subjected to various treatments. For Al treatment, 30 μM $AlCl_3$ was added to 0.5 mM $CaCl_2$ (pH 4.3). To evaluate the effects of reactive aldehydes on root growth, 25, 50, 100, and 200 μM HE (dissolved in dimethyl sulfoxide) and 0.25, 0.5, 1, 2.5, and 5 mM carnosine (CS) were added to 0.5 mM $CaCl_2$ (pH 4.3). Each experiment was repeated thrice.

Root Elongation Analysis. The primary root length of 20 roots was measured with a ruler before and after exposure to different treatments for 24 h. Relative root elongation was calculated as the percentage of the elongation values under different treatments compared with the elongation values under the control treatment.

Cell Membrane Integrity Visualization and Determination. Cell membrane integrity was detected by staining with Evans blue solution (0.25%, w/v) for 20 min and observed under a stereoscopic microscope (Nikon SMZ800N). After staining, the detained Evans blue solution in root tips was eluted by violent shaking in 5 mL of *N*,*N*-dimethylformamide. The optical density was determined spectrophotometrically at 600 nm as described in studies by Yamamoto *et al.* (2001).[31]

Aldehyde Detection and Quantification. Wheat seedlings were treated with 0 or 30 μM $AlCl_3$ for 24 h. Root tips (0−10 mm) were used to visualize aldehyde distribution after staining with Schiff's reagent (Sigma-Aldrich).[31] The roots were stained with Schiff's reagent for 20 min and rinsed with potassium metabisulfite solution (0.5%, w/v, dissolved in 0.05 M HCl) to retain the staining color. After staining, the roots were imaged under a microscope.

Approximately 0.3 g of root tips (0−10 mm) of seedlings was used for aldehyde quantitative analyses. Aldehydes were extracted from roots and derivated with 2,4-dinitrophenylhydrazine (DNPH) according to studies by Mano *et al.*,[35] with a slight modification. Briefly, the root tips were prepared and placed in 10 mL centrifuge tubes, and 2.5 mL of extract solution containing 10 μM 2-ethylhexanal (as an internal standard) and 0.005% (w/v) butylhydroxytoluene was added. Tissue homogenate was obtained via a grinding mechanism and incubated at 60 °C for 30 min. The extract was transferred into a new 10 mL centrifuge tube, and 62.5 μL of 20 mM DNPH and 48.4 μL of formic acid were added and thoroughly mixed. After incubation at 25 °C for 60 min, 2.5 mL of saturated NaCl solution and 0.45 g of $NaHCO_3$ were added to neutralize the formic acid. After centrifugation, the upper acetonitrile layer was collected in glass centrifuge tubes and evaporated to dryness in nitrogen. The residue was dissolved in 250 μL of acetonitrile. The sample solution was loaded on a BondElute C18 cartridge (Agilent) preconditioned with 1 mL of acetonitrile. The eluate was collected and subjected to HPLC-MS/MS. LC separation was performed using Agilent Technologies Agilent 1290 Infinity (Agilent Technologies. Santa Clara, California, USA). Fourteen species of aldehyde-DNPH derivatives were simultaneously chromatographed on a Zorbax SB-C18 column (2.1 × 150 mm, 3.5 μm, Agilent Technologies. Santa Clara, California, USA) at a column temperature of 40 °C. The mobile phases were aqueous solutions containing 5 mM ammonium acetate, 0.1% formic acid (A), and 0.1% methanol in acetonitrile (B). The following linear gradient programs were used (in reference to mobile phase A): 0−2 min, 60−55%; 2−30 min, 55−15%; 30−35 min, 15%; 35−38 min, 15−5%; 38−40 min, 5%; 40−41 min, 5−60%; and 41−45 min, 60%. The flow rate was 0.3 mL min^{-1}, and the sample injection volume was 20 μL. MS detection was performed on Agilent Technologies 6460 Triple Quad LC/MS (Agilent Technologies. Santa Clara, California, USA) with multiple reaction monitoring. The instrument was operated in negative mode to produce $[M - H]^-$ ions. The following ion source parameters were used: a gas temperature of 325 °C, a gas flow of 5 L/min, a nebulizer of 45 psi, a sheath gas temperature of 350 °C, a sheath gas flow of 11 L/min, a capillary voltage of 3000 V (positive) and 3500 V (negative), and a nozzle voltage of 500 V (negative). Data acquisition and analyses were performed using HPLC−MS/MS Quantitative Analysis Software B.07.00 1.6.1 (Agilent Technologies. Santa Clara, California, USA).

Electrolyte Leakage Assay. The loss of plasma membrane integrity was detected by measuring changes in electrical conductivity, as described in studies by Vemanna *et al.*[20] Root tips (0.15 g, 0−10 mm) were incubated in 30 mL of distilled water at 25 °C for 3 h. The initial electrical conductivity (E1) was measured when the solution was thoroughly mixed. Tubes were placed in a boiling water bath for 30 min, cooled at 25 °C, and mixed well, and the electrical conductivity was measured again (E2). The electrolyte leakage (EL) was calculated using the following formula: EL (%) = E1/E2 × 100.

Root Callose Determination. The callose content was measured as described in the study by Chen *et al.*[28] Approximately 50 mg of root tips was cut and immersed in 98% ethanol overnight and then transferred to 400 μL of 1 M NaOH and thoroughly homogenized. The homogenates were heated at 85 °C for 15 min. After centrifugation, an aliquot of 71 μL of the supernatant was mixed with 142 μL of aniline blue (0.1% w/v), 75 μL of HCl (1 M), and 210 μL of glycine−NaOH buffer (1 M; pH 9.5). After incubation at 50 °C for 20 min, the mixture was measured on a Spectra Max i3x microplate reader (Molecular Devices, Sunnyvale, CA, USA) at 400 nm excitation and 510 nm emission.

Protein Carbonyl Determination. The root tips were thoroughly homogenized using 2 mL of phosphate buffer solution (25 mM, pH 7.0). 1 mL of the supernatant was reacted with 400 μL of 10 mM DNPH (dissolved in 2 M HCl) for 1 h under dark conditions. Then, 500 μL of 0.2 g mL^{-1} trichloroacetic acid was added. After centrifugation at 12,000*g* and 4 °C for 15 min, the supernatant was discarded, and the pellets were washed twice with 1 mL of ethanol/ethyl

https://doi.org/10.1021/acs.jafc.1c03975
J. Agric. Food Chem. 2021, 69, 10496−10505

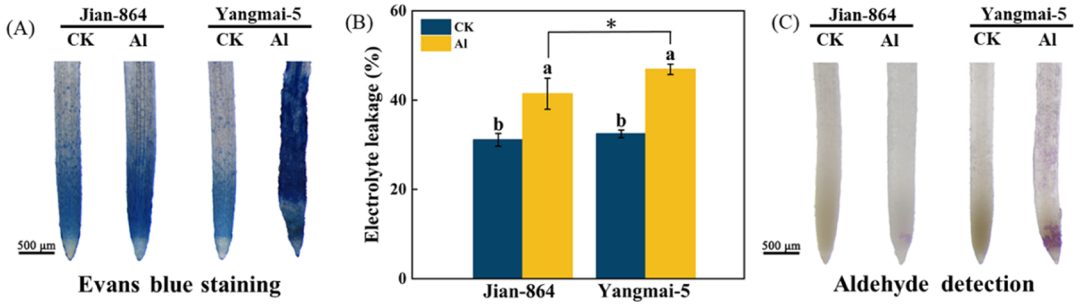

Figure 1. Effect of Al on roots of wheat seedlings. 3 day old seedlings were treated with or without 30 μM Al for 24 h. (A) Root tips of 10 biologically independent samples were excised for visualization of membrane damage using Evans blue staining. Scale bar = 500 μm. (B) Determination of EL. The data shown in the graph are the means ± SD (n = 3). (C) Schiff's reagent staining for determination of aldehydes. n = 10. Scale bar = 500 μm. Different letters in part (B) indicate statistically significant differences ($p < 0.05$). An asterisk (*) indicates a significant difference between genotypes.

acetate (v/v = 1/1). An aliquot of 1.25 mL of 6 M guanidine hydrochloride was added to the tubes. After incubation at 37 °C for 15 min, the mixture was centrifuged, and the supernatant was measured at 530 nm.

ROS Detection. The total ROS in root tips was monitored using 2,7-dichlorodihydrofluorescein diacetate (DCFH-DA) (Beyotime, Jiangsu, China). Briefly, the root tips were stained with 10 mM DCFH-DA for 20 min in the dark and rinsed in 10 mM PBS buffer (pH 7.4) at least twice. The stained root tips were visualized and captured using a Nikon Eclipse Ni fluorescence microscope. The intensities of green fluorescence of roots were analyzed using ImageJ software.

The content of H_2O_2 was determined as described in the study by Chen *et al.*[28] The root tips (0−10 mm, 0.1 g) were frozen in liquid nitrogen and homogenized with 2 mL of 0.1% (w/v) trichloroacetic acid. The homogenate was centrifuged at 12,000*g* for 15 min at 4 °C, and 0.5 mL of the supernatant was added to 0.5 mL of 10 mM potassium phosphate buffer (pH 7.0) and 1 mL of 1 M KI. The absorbance of the supernatant was measured at 390 nm. The content of H_2O_2 was calculated using a standard curve plotted with a known concentration of H_2O_2.

The O_2^- contents were measured as described in studies by Chen *et al.*[28] with slight modification. The root tips (0−10 mm, 0.1 g) were homogenized in 1.5 mL of phosphate buffer (50 mM, pH 7.8) and centrifuged at 12,000*g* for 20 min at 4 °C. An aliquot of 0.5 mL of the supernatant was mixed with 0.5 mL of 50 mM phosphate buffer (pH 7.8) and 0.1 mL of 10 mM hydroxylamine hydrochloride solution. The mixture was placed at 25 °C for 25 min. One milliliter of sulfanilamide and 1 mL of α-naphthylamine were added. The mixture was placed at 25 °C for 30 min, and the absorbance was determined at 540 nm. Sodium nitrite was used as the standard curve for the calculation of the O_2^- content.

Cell Death Detection. Cell death was detected using propidium iodide (PI). The root tips were sliced and treated with 10 μg/mL PI in the dark for 5 min and rinsed with deionized water at least twice. The roots were observed using a fluorescence microscope and photographed.

ALE Quantification. ALEs were measured using an ELISA kit (Shanghai Hengyuan Biotech, China). Approximately 0.1 g of fresh roots was frozen in liquid nitrogen and extracted with 0.9 mL of sodium phosphate buffer (50 mM, pH 7.0). After centrifugation, the supernatant was used to measure ALE contents by following the manufacturer's instructions.

Determination of Aldehyde Detoxifying Enzyme Activities. Approximately 0.1 g of root tips (0−10 mm) was homogenized in 0.9 mL of 50 mM sodium phosphate buffer (pH 7.0), and the extracts were centrifuged at 10,000*g* at 4 °C for 10 min. The crude extracts were used to determine the activities of alkenal reductase (AER), aldo-keto reductase (AKR), and alkenal/alkenone (AOR). For AER assay, 100 μL of the filtrates was added to a 900 μL reaction system including 0.1 mM nicotinamide adenine dinucleotide phosphate (NADPH) and 0.1 mM diamide (dissolved in 50 mM MES−NaOH buffer at pH 6.0). The AER activity was determined by the oxidation rate of NADPH at 340 nm. AKR was detected using ELISA kits (JL46485, Jianglai Biotechnology Co. Ltd., Shanghai, China). To assay the activity of AOR, an aliquot of 100 μL of the crude enzyme extract was mixed with 900 μL of 20 mM 3-buten-2-one in 50 mM sodium phosphate buffer (pH 7.0). NADPH was added to a final concentration of 0.1 mM and detected at 340 nm. Total soluble protein was determined by Coomassie brilliant blue, and bovine serum albumin was used as a standard.[28]

Gene Expression Analysis. The total RNA of root tips was extracted using a Spin Column Plant Total RNA Purification Kit (Sangon Biotech Co., Ltd, Shanghai, China). Total RNA was transferred to cDNA using HiScript II Q RT SuperMix (Vazyme Biotech Co., Ltd., Nanjing, China) in a 20 μL reaction volume. The reaction mixture contained 1000 ng of purified RNA. Quantitative real-time PCR analysis was performed with ChamQ SYBR Color qPCR Master Mix (Vazyme Biotech Co., Ltd., Nanjing, China) using a Light Cycler 480 II real-time PCR detection system (Roche, Rotkreuz, Switzerland). The relative transcript levels of *TaAKR1*, *TaAKR2*, *TaAOR*, and *TaAER* were determined and calculated using the $2^{-\Delta\Delta Ct}$ formula.[36] The wheat phosphogluconate dehydrogenase gene *Ta3079* was used as an internal control. The primer sequences of these genes are listed in Table S1 in Supporting Information.

Statistical Analysis. All data were statistically analyzed using SPSS 20.0 (SPSS Inc., Chicago, USA). All data were processed using analysis of variance, and mean separation was performed using one-way analysis of variance at $P < 0.05$ levels. The figures were plotted using OriginPro 2018 SR1 b9.5.1.195 (OriginLab Corporation, Northampton, USA).

RESULTS

Al-Induced Membrane Damage and Lipid Peroxidation in Wheat Roots. The loss of plasma membrane integrity was monitored using Evans blue staining. Roots treated with 30 μM $AlCl_3$ suffered severe cell death and membrane damage, especially the sensitive genotype Yangmai-5 (Figure 1A). This result was further confirmed using EL. The degree of EL was 1.2-fold higher in the roots of the sensitive genotype than the tolerant genotype (Figure 1B). The extensive enhancement of lipid damage was accompanied by a remarkable increase in aldehydes in wheat roots. After Al treatment, the presence of aldehydes in roots of Yangmai-5 was significantly enhanced in a rapid test with Schiff's reagent (Figure 1C). These results suggest that Al caused oxidative damage and lipid peroxidation, which led to the formation of aldehydes sourced from lipid peroxide in wheat roots.

Reactive Aldehyde Profiling of Wheat Roots under Al Stress. To investigate the alterations of lipid peroxide-derived aldehydes, global profiling of aldehydes was separated and characterized using UPLC-QTOF-HRMS and UPLC-QqQ-MS/MS after DNPH derivatization (Tables S2 and S3). Based on standards, fragmentation patterns in the literature or database, retention time, and dozens of aldehydes sourced

https://doi.org/10.1021/acs.jafc.1c03975
J. Agric. Food Chem. 2021, 69, 10496−10505

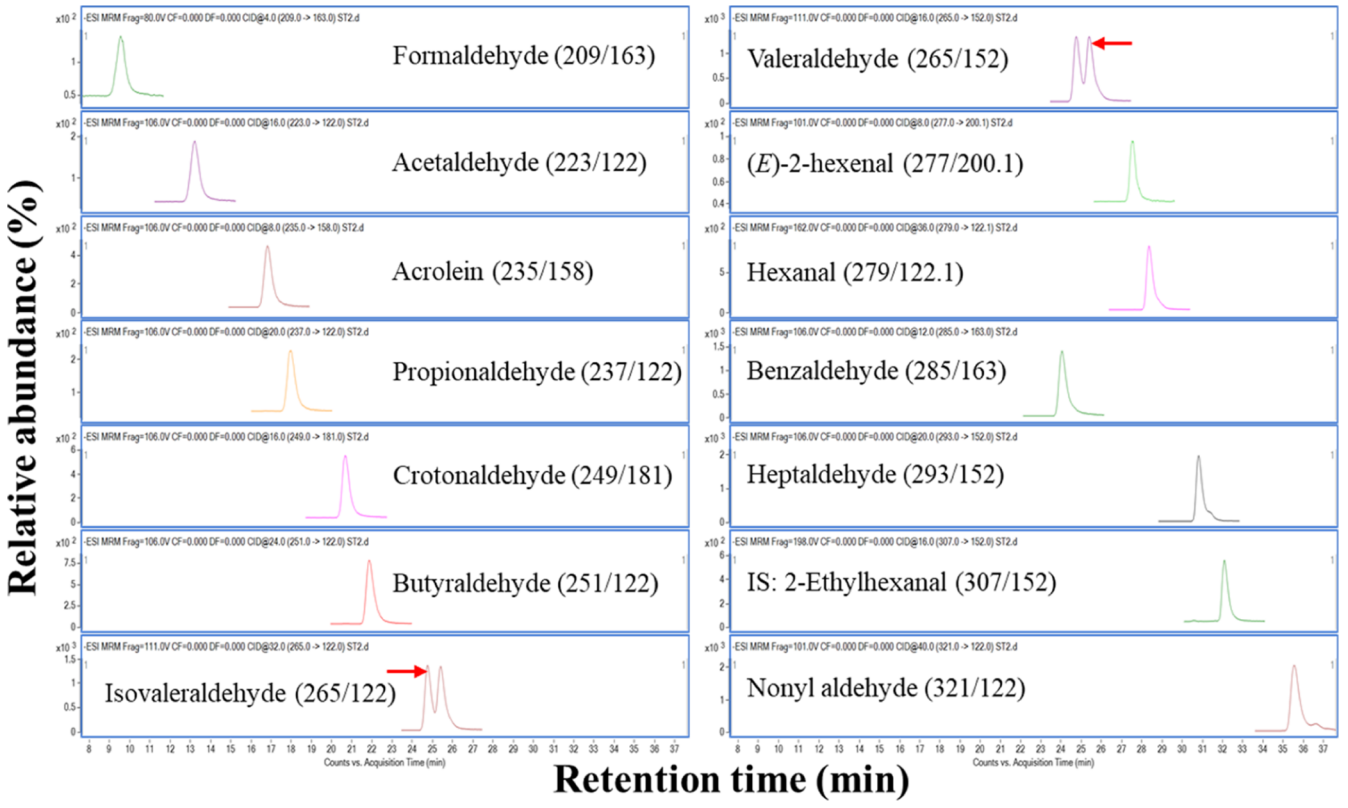

Figure 2. Extraction ion chromatograms and 14 species of aldehyde standard DNPH derivatives using HPLC−MS/MS; IS: internal standard.

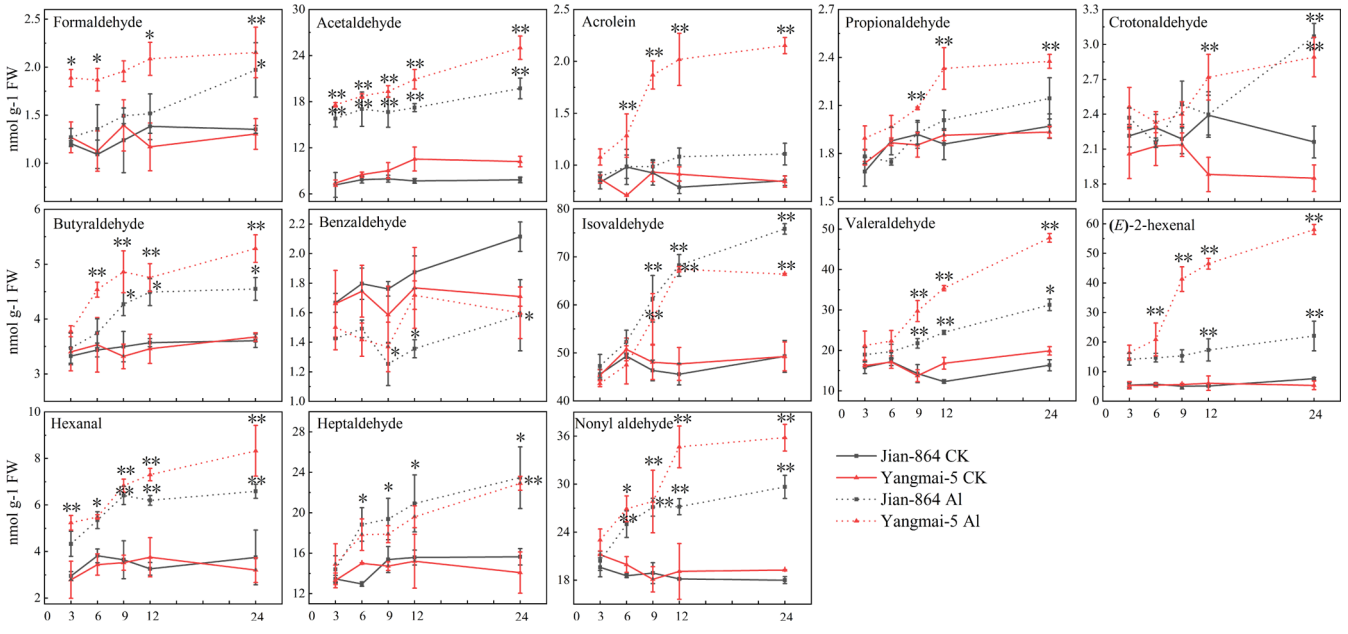

Figure 3. Aldehyde content in wheat roots quantified using HPLC−MS/MS. The root tips of 3 day old seedlings treated with or without 30 μM $AlCl_3$ for 24 h were excised at 3, 6, 9, 12, and 24 h for aldehyde content determination. The data shown are the means ± SD (n = 3). * and ** indicate significant differences at $p < 0.05$ and $p < 0.01$, respectively, between the control and Al treatment for the two genotypes at each time point.

from lipids in wheat roots were identified (Table S2). Among the identified aldehydes, the kinetics of 13 candidate species for the damage-causing molecules, generally with highly reactive 2-alkenals or short carbon chains, were further quantified and compared in Yangmai-5 and Jian-864 at different time points. As shown in Figure 2, all of the selected reactive aldehydes were elucidated after DNPH derivatization and separated well, except isovaleraldehyde and valeraldehyde.

The levels of several lipid peroxide-derived aldehydes, including acetaldehyde, HE, and hexanal, were elevated in wheat roots after 6 h of Al exposure, and the abundance increased with the extended Al stress time, especially in the sensitive genotype (Figure 3). Among the 13 candidates,

https://doi.org/10.1021/acs.jafc.1c03975
J. Agric. Food Chem. 2021, 69, 10496−10505

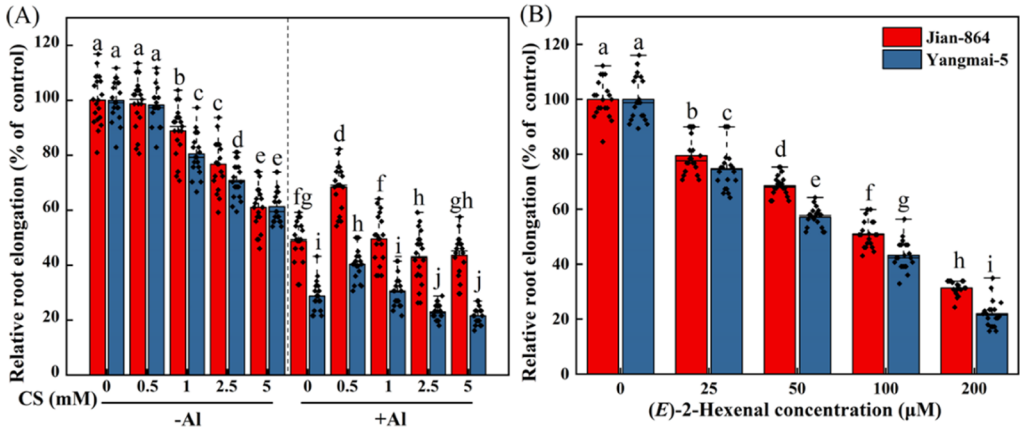

Figure 4. Effects of HE and CS on root growth. Three day old seedlings were treated with 0, 0.5, 1, 2.5, or 5 mM CS with or without 30 μM Al for 24 h (A) and 0, 25, 50, 100, or 200 μM HE (B) with 30 μM Al for 24 h. The relative root elongation was calculated. The data shown are the means ± SD (n = 20). Values followed by different letters are significantly different, and the same letter is not significantly different at $p < 0.05$.

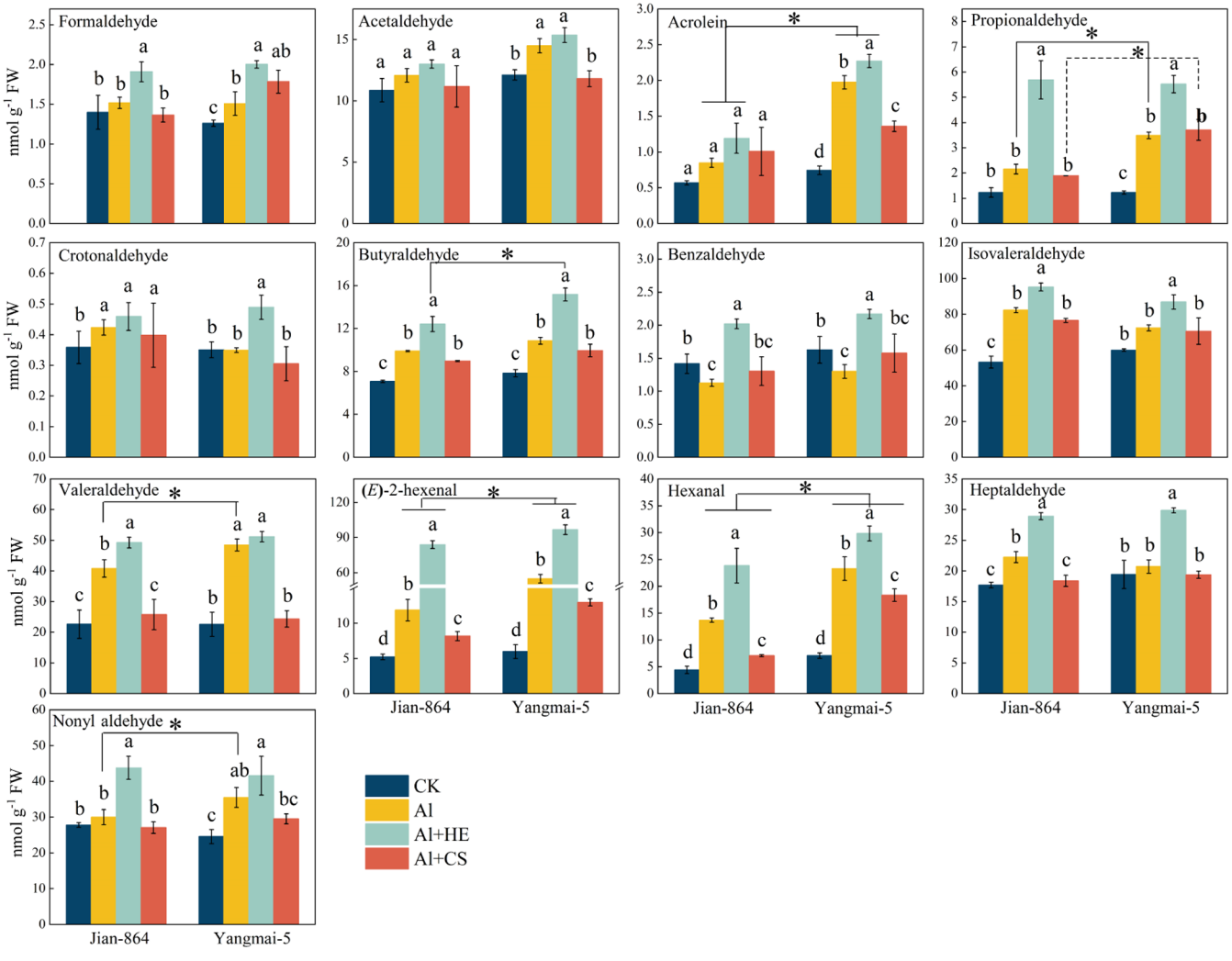

Figure 5. Aldehyde content in root tips (0−10 mm) of 3 day old wheat seedlings treated with the following solutions: (1) 0.5 mm $CaCl_2$ solution (CK), (2) 0.5 mm $CaCl_2$ + 30 μM $AlCl_3$, (3) 0.5 mm $CaCl_2$ + 30 μM $AlCl_3$ + 50 μM HE, and (4) 0.5 mm $CaCl_2$ + 30 μM $AlCl_3$ + 0.5 mM CS for 24 h. Data shown are the means ± SD (n = 3). Different letters indicate significant differences at $p < 0.05$. An asterisk (*) indicates a significant difference between genotypes.

acetaldehyde, isovaldehyde, valeraldehyde, HE, heptaldehyde, and nonyl aldehyde were the predominant species, and their contents were more than 10 nmol/g in the roots of both wheat genotypes after Al treatment. In contrast, the other candidates were present in small amounts (Figure 3). Most of the short-carbon chain aldehydes presented the highest amounts after 24 h

https://doi.org/10.1021/acs.jafc.1c03975
J. Agric. Food Chem. 2021, 69, 10496−10505

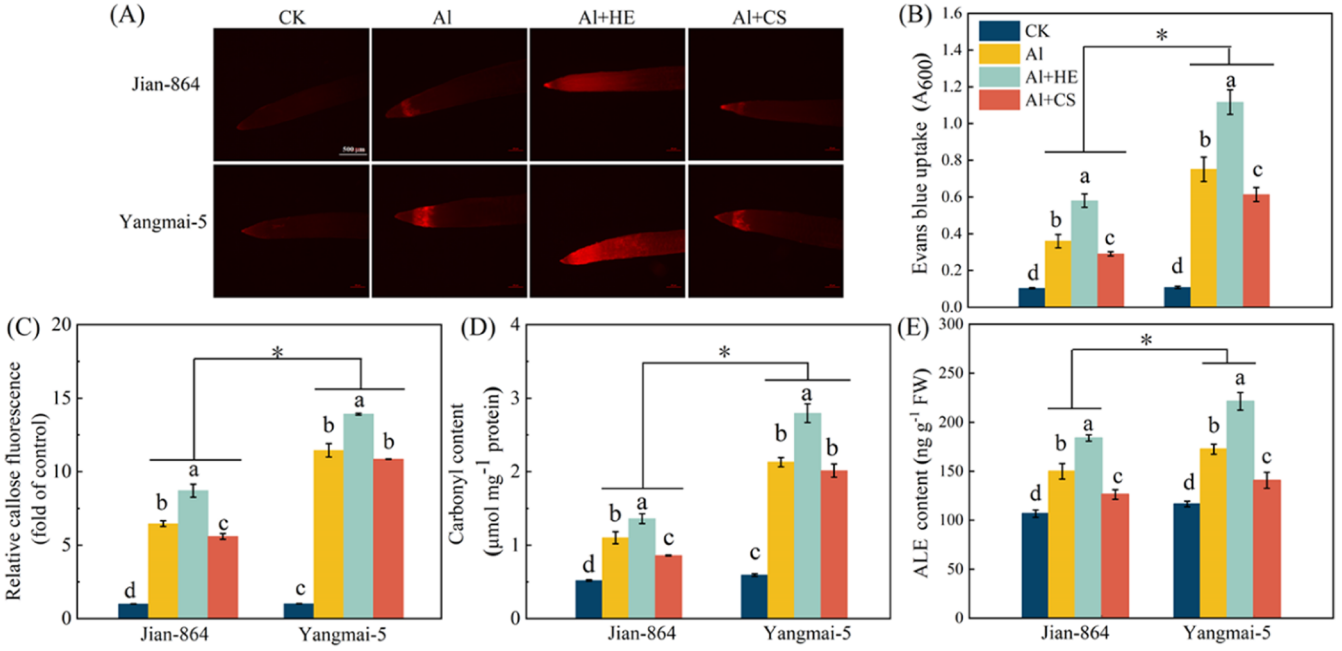

Figure 6. Effect of aldehydes on cell death (A), integrity of the cell membrane (B), callose content (C), protein carbonyl content (D), and ALEs (E) of 0−10 mm root tips. Three day old wheat root tips were treated with the following solutions: (1) 0.5 mm $CaCl_2$ solution (CK), (2) 0.5 mm $CaCl_2$ + 30 μM $AlCl_3$, (3) 0.5 mm $CaCl_2$ + 30 μM $AlCl_3$ + 50 μM HE, and (4) 0.5 mm $CaCl_2$ + 30 μM $AlCl_3$ + 0.5 mM CS for 24 h. For determination of cell death by PI, root tips from 10 biologically independent samples were used. Scale bar = 500 μm. Data shown in the graph (B−E) are the means ± SD (n = 3). Different letters indicate significant differences at $p < 0.05$. An asterisk (*) indicates a significant difference between genotypes.

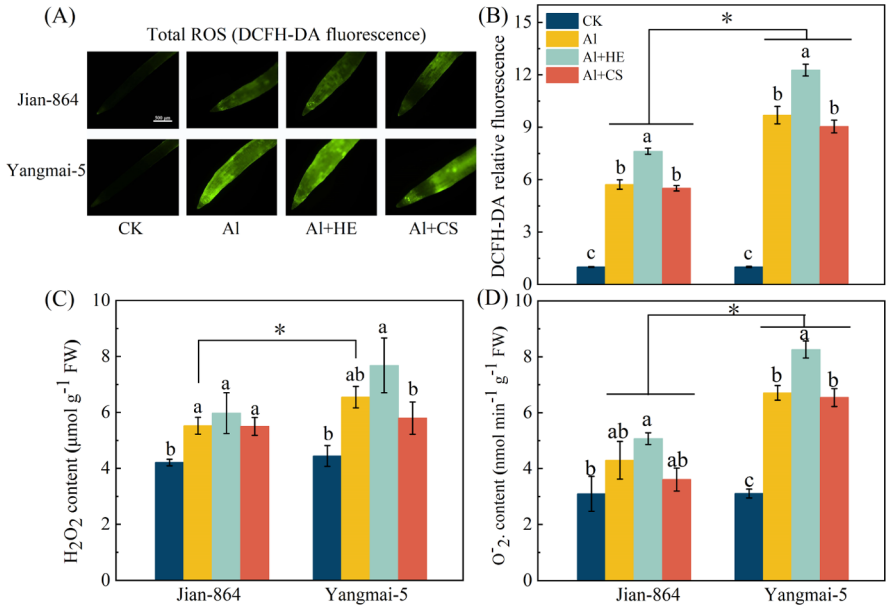

Figure 7. Effect of the carbonyl scavenger CS on ROS accumulation in wheat root tips. Three day old wheat root tips (0−10 mm) were treated with the following solutions: (1) 0.5 mm $CaCl_2$ solution (CK), (2) 0.5 mm $CaCl_2$ + 30 μM $AlCl_3$, (3) 0.5 mm $CaCl_2$ + 30 μM $AlCl_3$ + 50 μM HE, and (4) 0.5 mm $CaCl_2$ + 30 μM $AlCl_3$ + 0.5 mM CS for 24 h. For fluorescence staining of ROS, root tips from 10 biologically independent samples were used. Scale bar = 500 μm. Data shown are the means ± SD (n = 3). Different letters indicate significant differences at $p < 0.05$. An asterisk (*) indicates a significant difference between genotypes.

when root growth also showed severe inhibition during the treatment period (Figure S1). Both genotypes accumulated high levels of acetaldehyde, crotonaldehyde, isovaleraldehyde, valeraldehyde, HE, hexanal, heptanal, and nonanal. However, the relative abundances of acrolein and HE in the sensitive genotype were more than 1.94 and 2.63 times higher than the levels in the tolerant genotype, respectively (Figure 3). These results indicate that specific lipid peroxide-derived short-carbon chain aldehydes, such as HE and acrolein, which increased significantly in the sensitive genotype, are likely involved in Al phytotoxicity in wheat roots.

Effect of Aldehyde on Root Growth under Al Stress. To test whether lipid peroxide-derived aldehydes were involved in Al-triggered root growth inhibition, a specific and effective aldehyde-scavenging agent, CS, was used. A range of concentrations was tested, and it was found that 0.5 mM CS

https://doi.org/10.1021/acs.jafc.1c03975
J. Agric. Food Chem. 2021, 69, 10496−10505

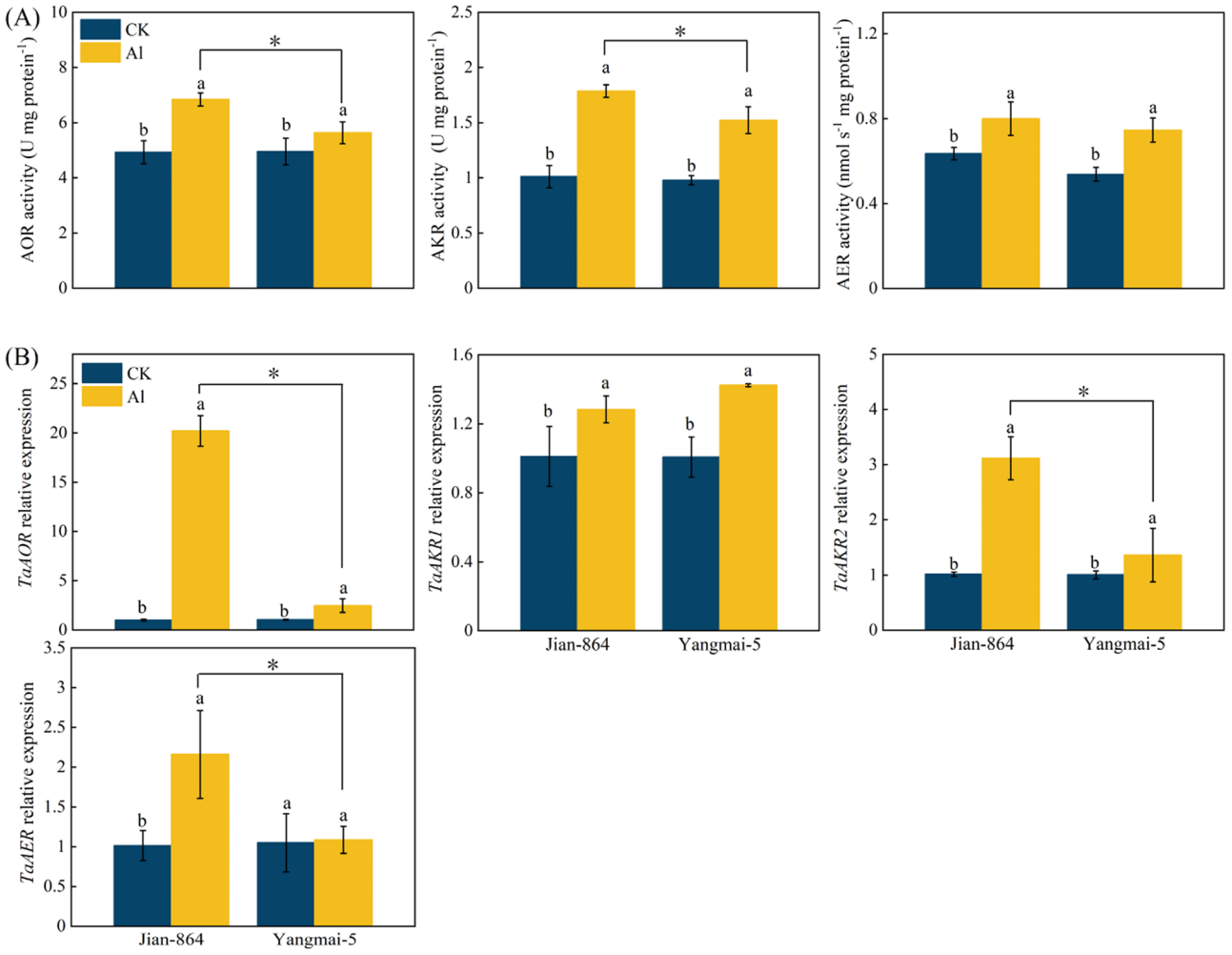

Figure 8. Effect of Al on aldehyde-detoxifying enzymes AOR, AKR, and AER (A) and aldehyde-detoxifying enzyme gene expression (B). The data shown are the means ± SD ($n = 3$). Different letters indicate significant differences at $p < 0.05$. An asterisk (*) indicates a significant difference between genotypes.

increased root growth by 19.59 and 11.63% in Jian-864 and Yangmai-5, respectively, under Al stress (Figure 4A). However, other selected concentrations showed nonalleviating or detrimental effects on wheat roots in the presence or absence of Al. These results indicated that aldehydes sourced from lipids mediated root growth inhibition under Al stress in wheat plants. The toxicity of lipid peroxide-derived aldehydes was confirmed by the exogenous application of HE, which was the most abundant and significantly different aldehyde species between Yangmai-5 and Jian-864. Treatment with HE for 24 h significantly inhibited root growth in both wheat genotypes in a dose-dependent manner. The relative root elongation of wheat decreased after treatment with 25, 50, 100, and 200 μM HE by 20.53, 31.44, 48.95, and 68.63% in Jian-864 and 25.21, 42.60, 56.77, and 78.02% in Yangmai-5, respectively (Figure 4B). A 50 μM HE treatment was selected for subsequent experiments because this concentration resulted in moderate root inhibition and a significant difference in the relative root elongation rate between the two genotypes.

Effect of Aldehyde and CS on Al-Induced Cell Damage. Among the identified short-carbon chain aldehydes, especially valeraldehyde, HE, and hexenal, CS application significantly decreased in abundance (Figure 5). CS mitigated Al-induced cell death, as indicated *in situ* by the fluorescent probe PI (Figure 6A). Compared to Al treatment, Al + CS treatment retained membrane integrity and protein oxidation by 19.16 and 18.31% in Jian-864 and 21.74 and 5.43% in Yangmai-5 (Figure 6B,D). In addition to promoting root growth, the application of CS significantly decreased callose deposition, which is another typical symptom of Al phytotoxicity (Figure 6C), and the content of ALEs also displayed a remarkable decrease in both wheat genotypes (Figure 6E). *In situ* monitoring of total ROS in roots using the green fluorescent probe DCFH-DA and chemical determination of H_2O_2 and O_2^- showed that CS did not significantly influence ROS levels (Figure 7), which indicates that the resulting short-carbon chain aldehydes exacerbated Al toxicity in wheat plants downstream of ROS.

In contrast, the degrees of aldehyde accumulation, cell death, membrane damage, and protein oxidation were further enhanced under Al stress after 50 μM HE treatment. However, wheat roots treated with HE showed elevated ROS under Al treatment (Figure 7), which suggests that aldehydes exacerbate cell injury via loop-mediated oxidative stress amplification.

Detoxifying Enzymes Contribute to Al Tolerance. The activities of three aldehyde detoxifying enzymes, AOR, AKR, and AER, were determined (Figure 8A). The results showed that Al stress significantly induced the detoxifying capacity of these enzymes in the two wheat genotypes, and Jian-864 exhibited

https://doi.org/10.1021/acs.jafc.1c03975
J. Agric. Food Chem. 2021, 69, 10496−10505

stronger aldehyde detoxifying enzyme activity than Yangmai-5. The expression of *TaAOR* extensively increased by 20.21 times in Jian-864 but only increased by 2.47-fold in Yangmai-5. We found that Al also induced the transcription of two encoding genes of AKR, *TaAKR1*, and *TaAKR2*. The relative expression of *TaAKR1* showed no significant difference between the two wheat genotypes, but the relative expression of *TaAKR2* in Jian-864 was 2.29 times higher than that in Yangmai-5 after Al treatment (Figure 8B). Al significantly improved the expression of *TaAER* coding AER, while it had little influence on Yangmai-5 (Figure 8B).

DISCUSSION

Oxidative injury of root cells has been recognized as a primary event during Al toxicity in plants.[1,5,37] In the present study, we found that Al toxicity resulted in a significant increase in ROS in wheat roots, especially in the sensitive wheat genotype (Figure 7). We also found that the overaccumulation of ROS in the Al-sensitive genotype correlated well with the obvious formation of reactive aldehyde compounds (Figure 1C). These results are similar to results reported in pineapple,[27] pea,[31] and wheat roots[4] and implicate that oxidative damage might be due to Al toxicity in plant roots.

Lipid peroxide-derived aldehydes contribute significantly to Al phytotoxicity in wheat plants. The increased accumulation of cellular aldehydes in plants inhibited seed germination, induced programmed cell death, and inhibited root development.[38−41] Several lines of evidence in the present study suggest that lipid peroxide-derived aldehydes mediate Al-induced injury of wheat roots. Exogenous application of aldehyde resulted in an increase in endogenous intercellular aldehyde levels, followed by severe cell damage and root growth inhibition in both genotypes (Figures 5 and 4B). Application of CS, an effective aldehyde-scavenging agent, significantly eliminated intracellular aldehyde accumulation (Figure 5), thereby alleviating the oxidative injury and inhibition of root elongation, especially in the sensitive genotype Yangmai-5 (Figures 6 and 4). A close relationship between lipid peroxide-derived aldehydes and cellular injury was characterized in plants under adverse conditions, such as drought,[26] salt,[26] high temperatures,[42] and nutrient deficiency.[22] For example, cytotoxic aldehydes sourced from lipids, such as MDA, significantly accumulated in tobacco plants under salt stress, which affected the function of many enzymes.[20] Similarly, Mano *et al.* also reported that lipid peroxide-derived α,β-unsaturated aldehydes in *Arabidopsis* leaves increased significantly under salt stress, and a unique set of proteins were sensitive to these aldehydes.[43] Under heat stress, MDA sourced from linolenic acids caused protein modification and inhibited the Rubisco activity.[42] However, it must be noted that CS introduced in this study did not affect Al-induced ROS levels, and the exogenous application of aldehyde further elevated ROS contents under Al treatment (Figure 4A). Previous studies and the present study indicated that the excessive accumulation of aldehydes exacerbated stress toxicity to plants downstream of ROS and may propagate oxidative stress via loop-mediated amplification.

The predominance of certain lipid peroxide-derived short-carbon chain aldehydes observed in wheat roots may be responsible for root injury under Al stress. Previous studies reported increased total aldehyde compounds under Al treatment,[4,31] but few studies investigated global aldehyde fragments generated from different fatty acid peroxides, which have distinct biological activities. Under salt stress, Mano *et al.* proposed that α,β-unsaturated aldehydes sourced from lipids strongly inactivated a unique set of proteins and exacerbated the tissue injury in *Arabidopsis* leaves.[43] It has been found that HNE, but not MDA, was associated with Al stress in barley roots.[34] The current study identified dozens of aldehydes sourced from lipids in wheat roots after derivatization (Table S2). In the case of aldehydes with a short length of carbon chains are potent electrophiles that trigger indiscriminate damage to cellular macromolecules in plants. Biswas and Mano systematically identified that lipid peroxide-derived short-carbon chain carbonyls, such as HNE and acrolein, mediated programmed cell death in oxidatively stressed tobacco Bright Yellow-2 cells.[39] Here, we detected and characterized 13 candidate species with short carbon chains. Consistent with Schiff's staining, chromatographic results showed that the sensitive genotype Yangmai-5 accumulated higher levels of short-chain aldehydes, such as acrolein, propionaldehyde, valeraldehyde, HE, hexanal, and nonyl aldehyde, than the tolerant genotype Jian-864 (Figure 5). The complementary results of the differences in aldehyde kinetics and CS effects between Yangmai-5 and Jian-864 suggest that these lipid peroxide-derived short-carbon chain aldehydes may mediate Al toxicity in wheat plants.

Among the resulting short-chain aldehydes, HE was the predominant species and had a strong positive relationship with lipid peroxidation and Al-induced root growth inhibition. With the specific structure, HE belonging to α,β-unsaturated aldehyde has strong electrophiles and cytotoxicity by forming Michael adducts and Schiff bases with proteins and nucleic acids.[33,39] *In vitro*, α,β-unsaturated carbonyls inhibited thiol-regulated enzymes in chloroplasts and lipoate enzymes in mitochondria.[44,45] Intense illumination increased HE levels in plant chloroplasts and caused photoinhibition in tobacco leaves.[23] Our results showed that the relative abundance of HE in the roots of the sensitive genotype Yangmai-5 was more than 2.63 times higher than that in the tolerant genotype Jian-864 after 24 h of Al treatment (Figure 3). Exogenous HE application significantly exacerbated membrane damage and inhibited root growth in both wheat genotypes (Figures 6 and 4B). The inhibition of root elongation caused by HE was also reported in tobacco and *Arabidopsis*.[46,47] Together, these findings suggest that excessive HE plays a critical role in mediating plant cell injury under stress conditions.

Our investigation also suggests that maintaining cellular aldehyde homeostasis via related scavenging enzymes facilitates plant performance under Al stress. Many plant reductases, such as AER and AKR, can metabolize aldehydes, alleviating their cytotoxicity. For example, overproduction of the *AKR1* gene enhanced the seed longevity of tobacco and rice by decreasing MDA and methylglyoxal accumulation.[48] Upregulation of the *AER* expression improved maize adaption to low-nitrogen stress.[22] We found that Al stress substantially improved the activity of AOR, AKR, and AER and the expression of *TaAKR1*, *TaAKR2*, *TaAOR*, and *TaAER* in the two wheat genotypes, and Jian-864 showed a stronger capacity to control aldehyde homeostasis than Yangmai-5 (Figure 8). This result may explain why Jian-864 exhibited resistance to Al stress. These results are consistent with a study on tobacco, in which *AER* overexpression plants maintained lower aldehyde concentrations and showed stronger resistance against Al stress.[47] Our results, combined with previously published studies, suggest that aldehyde-detoxifying enzymes are particularly critical to plant development and responses to abiotic stress.

https://doi.org/10.1021/acs.jafc.1c03975
J. Agric. Food Chem. 2021, 69, 10496−10505

In summary, our study demonstrated that Al stress-induced ROS triggered lipid peroxidation and led to the formation of various reactive aldehyde compounds, which triggered indiscriminate damage to plant seedlings, especially in the Al-sensitive genotype. Our results also suggest that lipid peroxide-derived short-chain aldehydes exacerbate oxidative injury downstream of ROS and propagate oxidative stress via loop-mediated amplification. Furthermore, it was found that strong aldehyde-detoxifying capacity is necessary, or at least beneficial, for plant performance under Al stress. The present study may be extended to explore other possible pathways in addition to ROS-lipid peroxidation of toxic aldehyde production. The physiological and molecular mechanisms of aldehyde-induced Al toxicity should be investigated further.

■ ASSOCIATED CONTENT

Supporting Information

The Supporting Information is available free of charge at https://pubs.acs.org/doi/10.1021/acs.jafc.1c03975.

Relative root elongation rates at different times; qPCR primers for genes of wheat aldehyde-detoxifying enzymes; molecular weight, retention time, precursor ions, product ions, and collision energy of 14 species of aldehyde-DNPH derivatives; and identities of aldehyde-DNPH derivatives in wheat roots using UPLC-TOF-MS (PDF)

■ AUTHOR INFORMATION

Corresponding Author

Xianyong Lin − *MOE Key Laboratory of Environment Remediation and Ecological Health, College of Environmental & Resource Sciences, Zhejiang University, Hangzhou 310058, China;* orcid.org/0000-0002-9801-7008; Email: xylin@zju.edu.cn

Authors

Xin Liang − *MOE Key Laboratory of Environment Remediation and Ecological Health, College of Environmental & Resource Sciences, Zhejiang University, Hangzhou 310058, China*

Yiqun Ou − *MOE Key Laboratory of Environment Remediation and Ecological Health, College of Environmental & Resource Sciences, Zhejiang University, Hangzhou 310058, China*

Hongcheng Zhao − *MOE Key Laboratory of Environment Remediation and Ecological Health, College of Environmental & Resource Sciences, Zhejiang University, Hangzhou 310058, China*

Weiwei Zhou − *College of Resource and Environment, Qingdao Agricultural University, Qingdao 266000, China*

Chengliang Sun − *MOE Key Laboratory of Environment Remediation and Ecological Health, College of Environmental & Resource Sciences, Zhejiang University, Hangzhou 310058, China;* orcid.org/0000-0003-1399-6591

Complete contact information is available at: https://pubs.acs.org/10.1021/acs.jafc.1c03975

Notes

The authors declare no competing financial interest.

■ ACKNOWLEDGMENTS

This work was financially supported by the National Natural Science Foundation of China (31872167) and the Zhejiang Provincial Natural Science Foundation of China (LQ21C150007).

■ ABBREVIATIONS

Al, aluminum; HE, (*E*)-2-hexenal; ROS, reactive oxygen species; ALEs, advanced lipoxidation end products; HNE, 4-hydroxy-(*E*)-2-nonenal; MDA, malondialdehyde; CS, carnosine; DNPH, 2,4-dinitrophenylhydrazine; PI, propidium iodide; DCFH-DA, 2,7-dichlorodihydrofluorescein diacetate; EL, electrolyte leakage; ELISA, enzyme-linked immunosorbent assay; AER, alkenal reductase; AKR, aldo-keto reductase; AOR, alkenal/alkenone reductase; NADPH, nicotinamide adenine dinucleotide phosphate

■ REFERENCES

(1) Ma, J. F. Syndrome of aluminum toxicity and diversity of aluminum resistance in higher plants. *Int. Rev. Cytol.* **2007**, *264*, 225−252.

(2) Wang, P.; Dong, Y.; Zhu, L.; Hao, Z.; Hu, L.; Hu, X.; Wang, G.; Cheng, T.; Shi, J.; Chen, J. The role of gamma-aminobutyric acid in aluminum stress tolerance in a woody plant, Liriodendron chinense × tulipifera. *Hortic. Res.* **2021**, *8*, 80.

(3) Horst, W. J.; Wang, Y.; Eticha, D. The role of the root apoplast in aluminium-induced inhibition of root elongation and in aluminium resistance of plants: a review. *Ann. Bot.* **2010**, *106*, 185−197.

(4) Sun, C.; Liu, L.; Yu, Y.; Liu, W.; Lu, L.; Jin, C.; Lin, X. Nitric oxide alleviates aluminum-induced oxidative damage through regulating the ascorbate-glutathione cycle in roots of wheat. *J. Integr. Plant Biol.* **2015**, *57*, 550−561.

(5) Pereira, L. B.; Mazzanti, C. M. d. A.; Gonçalves, J. F.; Cargnelutti, D.; Tabaldi, L. A.; Becker, A. G.; Calgaroto, N. S.; Farias, J. G.; Battisti, V.; Bohrer, D.; Nicoloso, F. T.; Morsch, V. M.; Schetinger, M. R. C. Aluminum-induced oxidative stress in cucumber. *Plant Physiol. Biochem.* **2010**, *48*, 683−689.

(6) Chauhan, D. K.; Yadav, V.; Vaculík, M.; Gassmann, W.; Pike, S.; Arif, N.; Singh, V. P.; Deshmukh, R.; Sahi, S.; Tripathi, D. K. Aluminum toxicity and aluminum stress-induced physiological tolerance responses in higher plants. *Crit. Rev. Biotechnol.* **2021**, *41*, 715−730.

(7) Sun, C.; Liu, L.; Zhou, W.; Lu, L.; Jin, C.; Lin, X. Aluminum induces distinct changes in the metabolism of reactive oxygen and nitrogen species in the roots of two wheat genotypes with different aluminum resistance. *J. Agric. Food Chem.* **2017**, *65*, 9419−9427.

(8) Du, H.; Huang, Y.; Qu, M.; Li, Y.; Hu, X.; Yang, W.; Li, H.; He, W.; Ding, J.; Liu, C.; Gao, S.; Cao, M.; Lu, Y.; Zhang, S. A maize zmat6 gene confers aluminum tolerance via reactive oxygen species scavenging. *Front. Plant Sci.* **2020**, *11*, 1016.

(9) Mano, J. Reactive carbonyl species: their production from lipid peroxides, action in environmental stress, and the detoxification mechanism. *Plant Physiol. Biochem.* **2012**, *59*, 90−97.

(10) Parvez, S.; Long, M. J. C.; Poganik, J. R.; Aye, Y. Redox signaling by reactive electrophiles and oxidants. *Chem. Rev.* **2018**, *118*, 8798−8888.

(11) Yamamoto, Y.; Kobayashi, Y.; Devi, S. R.; Rikiishi, S.; Matsumoto, H. Aluminum toxicity is associated with mitochondrial dysfunction and the production of reactive oxygen species in plant cells. *Plant Physiol.* **2002**, *128*, 63−72.

(12) Gill, S. S.; Tuteja, N. Reactive oxygen species and antioxidant machinery in abiotic stress tolerance in crop plants. *Plant Physiol. Biochem.* **2010**, *48*, 909−930.

(13) Guéraud, F.; Atalay, M.; Bresgen, N.; Cipak, A.; Eckl, P. M.; Huc, L.; Jouanin, I.; Siems, W.; Uchida, K. Chemistry and biochemistry of lipid peroxidation products. *Free Radic. Res.* **2010**, *44*, 1098−1124.

(14) Ramu, V. S.; Preethi, V.; Nisarga, K. N.; Srivastava, K. R.; Sheshshayee, M. S.; Mysore, K. S.; Udayakumar, M. Carbonyl cytotoxicity affects plant cellular processes and detoxifying enzymes scavenge these compounds to improve stress tolerance. *J. Agric. Food Chem.* **2020**, *68*, 6237−6247.

(15) Pamplona, R. Advanced lipoxidation end-products. *Chem. Biol. Interact.* **2011**, *192*, 14−20.

(16) Mol, M.; Degani, G.; Coppa, C.; Baron, G.; Popolo, L.; Carini, M.; Aldini, G.; Vistoli, G.; Altomare, A. Advanced lipoxidation end products (ALEs) as RAGE binders: Mass spectrometric and computational studies to explain the reasons why. *Redox Biol.* **2019**, *23*, 101083.
(17) Alché, J. d. D. A concise appraisal of lipid oxidation and lipoxidation in higher plants. *Redox Biol.* **2019**, *23*, 101136.
(18) Alméras, E.; Stolz, S.; Vollenweider, S.; Reymond, P.; Mene-Saffrane, L.; Farmer, E. E. Reactive electrophile species activate defense gene expression in Arabidopsis. *Plant J.* **2003**, *34*, 202−216.
(19) Cruz de Carvalho, M. H. Drought stress and reactive oxygen species: Production, scavenging and signaling. *Plant Signal. Behav.* **2008**, *3*, 156−165.
(20) Vemanna, R. S.; Babitha, K. C.; Solanki, J. K.; Amarnatha Reddy, V.; Sarangi, S. K.; Udayakumar, M. Aldo-keto reductase-1 (AKR1) protect cellular enzymes from salt stress by detoxifying reactive cytotoxic compounds. *Plant Physiol. Biochem.* **2017**, *113*, 177−186.
(21) Zhao, J.; Missihoun, T. D.; Bartels, D. The role of Arabidopsis aldehyde dehydrogenase genes in response to high temperature and stress combinations. *J. Exp. Bot.* **2017**, *68*, 4295−4308.
(22) Wang, Y.; Zhao, Y.; Wang, S.; Liu, J.; Wang, X.; Han, Y.; Liu, F. Up-regulated 2-alkenal reductase expression improves low-nitrogen tolerance in maize by alleviating oxidative stress. *Plant Cell Environ.* **2020**, *44*, 559−573.
(23) Mano, J. i.; Tokushige, K.; Mizoguchi, H.; Fujii, H.; Khorobrykh, S. Accumulation of lipid peroxide-derived, toxic alpha,beta-unsaturated aldehydes (E)-2-pentenal, acrolein and (E)-2-hexenal in leaves under photoinhibitory illumination. *Plant Biotechnol.* **2010**, *27*, 193−197.
(24) Oberschall, A.; Deak, M.; Torok, K.; Sass, L.; Vass, I.; Kovacs, I.; Feher, A.; Dudits, D.; Horvath, G. V. A novel aldose/aldehyde reductase protects transgenic plants against lipid peroxidation under chemical and drought stresses. *Plant J.* **2000**, *24*, 437−446.
(25) Sunkar, R.; Bartels, D.; Kirch, H.-H. Overexpression of a stress-inducible aldehyde dehydrogenase gene from Arabidopsis thaliana in transgenic plants improves stress tolerance. *Plant J.* **2003**, *35*, 452−464.
(26) Rodrigues, S. M.; Andrade, M. O.; Gomes, A. P.; Damatta, F. M.; Baracat-Pereira, M. C.; Fontes, E. P. Arabidopsis and tobacco plants ectopically expressing the soybean antiquitin-like ALDH7 gene display enhanced tolerance to drought, salinity, and oxidative stress. *J. Exp. Bot.* **2006**, *57*, 1909−1918.
(27) Lin, Y.-H.; Chen, J.-H. Effects of aluminum on the cell morphology in the root apices of two pineapples with different Al-resistance characteristics. *Soil Sci. Plant Nutr.* **2019**, *65*, 353−357.
(28) Chen, Y.; Huang, L.; Liang, X.; Dai, P.; Zhang, Y.; Li, B.; Lin, X.; Sun, C. Enhancement of polyphenolic metabolism as an adaptive response of lettuce (Lactuca sativa) roots to aluminum stress. *Environ. Pollut.* **2020**, *261*, 114230.
(29) Giannakoula, A.; Moustakas, M.; Mylona, P.; Papadakis, I.; Yupsanis, T. Aluminum tolerance in maize is correlated with increased levels of mineral nutrients, carbohydrates and proline, and decreased levels of lipid peroxidation and Al accumulation. *J. Plant Physiol.* **2008**, *165*, 385−396.
(30) Ezaki, B.; Katsuhara, M.; Kawamura, M.; Matsumoto, H. Different mechanisms of four aluminum (Al)-resistant transgenes for Al toxicity in arabidopsis. *Plant Physiol.* **2001**, *127*, 918−927.
(31) Yamamoto, Y.; Kobayashi, Y.; Matsumoto, H. Lipid peroxidation is an early symptom triggered by aluminum, but not the primary cause of elongation inhibition in pea roots. *Plant Physiol.* **2001**, *125*, 199−208.
(32) Navascués, J.; Pérez-Rontomé, C.; Sánchez, D. H.; Staudinger, C.; Wienkoop, S.; Rellán-Álvarez, R.; Becana, M. Oxidative stress is a consequence, not a cause, of aluminum toxicity in the forage legume Lotus corniculatus. *New Phytol.* **2012**, *193*, 625−636.
(33) Mano, J.; Biswas, M. S.; Sugimoto, K. Reactive carbonyl species: a missing link in ros signaling. *Plants* **2019**, *8*, 391.
(34) Sakihama, Y.; Yamasaki, H. Lipid peroxidation induced by phenolics in conjunction with aluminum ions. *Biol. Plant* **2002**, *45*, 249−254.
(35) Mano, J. i.; Biswas, M. S. Analysis of reactive carbonyl species generated under oxidative stress. *Methods Mol. Biol.* **2018**, *1743*, 117−124.
(36) Majláth, I.; Éva, C.; Tajti, J.; Khalil, R.; Elsayed, N.; Darko, E.; Szalai, G.; Janda, T. Exogenous methylglyoxal enhances the reactive aldehyde detoxification capability and frost-hardiness of wheat. *Plant Physiol. Biochem.* **2020**, *149*, 75−85.
(37) Matsumoto, H.; Motoda, H. Oxidative stress is associated with aluminum toxicity recovery in apex of pea root. *Plant Soil* **2012**, *363*, 399−410.
(38) Shin, J.-H.; Kim, S.-R.; An, G. Rice aldehyde dehydrogenase7 is needed for seed maturation and viability. *Plant Physiol.* **2009**, *149*, 905−915.
(39) Biswas, M. S.; Mano, J. i. Lipid peroxide-derived short-chain carbonyls mediate hydrogen peroxide-induced and salt-induced programmed cell death in plants. *Plant Physiol.* **2015**, *168*, 885−898.
(40) Nisarga, K. N.; Vemanna, R. S.; Kodekallu Chandrashekar, B.; Rao, H.; Vennapusa, A. R.; Narasimaha, A.; Makarla, U.; Basavaiah, M. R. Aldo-ketoreductase 1 (AKR1) improves seed longevity in tobacco and rice by detoxifying reactive cytotoxic compounds generated during ageing. *Rice* **2017**, *10*, 11.
(41) Nareshkumar, A.; Subbarao, S.; Vennapusa, A. R.; Ashwin, V.; Banarjee, R.; Kulkarni, M. J.; Ramu, V. S.; Udayakumar, M. Enzymatic and non-enzymatic detoxification of reactive carbonyl compounds improves the oxidative stress tolerance in cucumber, tobacco and rice seedlings. *J. Plant Growth Regul.* **2020**, *39*, 1359−1372.
(42) Yamauchi, Y.; Furutera, A.; Seki, K.; Toyoda, Y.; Tanaka, K.; Sugimoto, Y. Malondialdehyde generated from peroxidized linolenic acid causes protein modification in heat-stressed plants. *Plant Physiol. Biochem.* **2008**, *46*, 786−793.
(43) Mano, J.; Nagata, M.; Okamura, S.; Shiraya, T.; Mitsui, T. Identification of oxidatively modified proteins in salt-stressed Arabidopsis: a carbonyl-targeted proteomics approach. *Plant Cell Physiol.* **2014**, *55*, 1233−1244.
(44) Taylor, N. L.; Day, D. A.; Millar, A. H. Environmental stress causes oxidative damage to plant mitochondria leading to inhibition of glycine decarboxylase. *J. Biol. Chem.* **2002**, *277*, 42663−42668.
(45) Mano, J. i.; Miyatake, F.; Hiraoka, E.; Tamoi, M. Evaluation of the toxicity of stress-related aldehydes to photosynthesis in chloroplasts. *Planta* **2009**, *230*, 639−648.
(46) Mirabella, R.; Rauwerda, H.; Struys, E. A.; Jakobs, C.; Triantaphylidès, C.; Haring, M. A.; Schuurink, R. C. The Arabidopsis her1 mutant implicates GABA in E-2-hexenal responsiveness. *Plant J.* **2008**, *53*, 197−213.
(47) Yin, L.; Mano, J. i.; Wang, S.; Tsuji, W.; Tanaka, K. The involvement of lipid peroxide-derived aldehydes in aluminum toxicity of tobacco roots. *Plant Physiol.* **2010**, *152*, 1406−1417.
(48) Turóczy, Z.; Kis, P.; Török, K.; Cserháti, M.; Lendvai, A.; Dudits, D.; Horváth, G. V. Overproduction of a rice aldo-keto reductase increases oxidative and heat stress tolerance by malondialdehyde and methylglyoxal detoxification. *Plant Mol. Biol.* **2011**, *75*, 399−412.

https://doi.org/10.1021/acs.jafc.1c03975
J. Agric. Food Chem. 2021, 69, 10496−10505